Genes & Diseases (2024) 11, 100982

Available online at www.sciencedirect.com

ScienceDirect

journal homepage: www.keaipublishing.com/en/journals/genes-diseases

RAPID COMMUNICATION

Transcriptomic and pathological profiling of a new congenic mouse model with *Lepr* mutation: Evaluating susceptibility to the development of obesity and NAFLD

Non-alcoholic fatty liver disease (NAFLD) and type 2 diabetes mellitus (T2DM) are two disease conditions for which obesity is a risk factor.[1] Due to the close relationship between the three pathologies, researchers frequently use the same mouse models to identify the underlying processes of obesity, NAFLD, and T2DM. For instance, leptin (*Lep*)-null (ob/ob) and leptin receptor (*Lepr*)-deficient (db/db) mice spontaneously develop NAFLD and show different phenotypes of extreme obesity and diabetes, respectively.[2,3] Creating and applying more pertinent models to analyze disease-specific pathways is necessary. Interestingly, wild-derived WSB/Eij mice are resistant to obesity and developing NAFLD. To comprehend the reason for this resistance and the potential role of the *Lepr* mutation in the development of obesity, we created the congenic strain WSB-db. These congenic WSB-db mice developed mild obesity and hyperglycemia without hepatic steatosis/NAFLD and renal consequences. Various differentially expressed genes (DEGs) were discovered in congenic WSB-db compared to its parent strains (WSB/Eij and B6-db), which may explain the different susceptibility to NAFLD. Thus, the congenic WSB-db mice may be a suitable model to separate the genes and mechanisms crucial to obesity and NAFLD.

We assessed the physiological parameters in the congenic and the two parental strains (B6-db/donor strain and WSB/recipient strain for the mutated *Lepr* gene). Despite the steady gain in body weight in all three strains at 44 weeks, the WSB-db mice (maximum average weight/MAW = 43 g) showed significantly increased weight, similar to the B6-db (MAW = 51 g), in comparison to the WSB mice (MAW = 18 g) (Fig. 1A, A′). Liver weight, measured in animals euthanized at the end of 8 weeks, exhibited a similar pattern to body weight where WSB-db and B6-db mice had a considerably higher liver weight compared to WSB mice" (Fig. 1B). *Lepr* mutation that causes starvation, possibly leads to increased average food intake/consumption in WSB-db, similar to B6-db, as compared to WSB mice (Fig. S1A), thus explaining the gain in body and liver weight due to overfeeding-induced adipose tissue deposition. Thus, the WSB-db congenic strain is susceptible to dietary obesity as opposed to the recipient parental strain.

Overall, the biochemical evaluation revealed no notable changes in serum biomarkers of WSB-db other than significantly higher cholesterol and triglyceride levels in WSB-db mice compared to both WSB and B6-db strains (Fig. 1C), which is possibly due to increased lipid synthesis. Blood glucose (Fig. 1D) and glycated hemoglobin (HbA1c, Fig. 1D′) levels, though elevated in WSB-db compared to the WSB strain, were substantially lesser than in the B6-db strain. The glucose tolerance test (Fig. 1E) and insulin tolerance test (Fig. 1E′) showed comparable trends of hyperglycemia and insulin resistance in both WSB-db and B6-db mice. Immunostaining of islets had greater expression of antibodies to insulin in WSB mice compared to WSB-db and B6-db mice. Thus, lesser expression of insulin in beta cells of pancreatic islets in WSB-db (Fig. S2C) suggests the model may be susceptible to diabetes. There were no significant changes in liver enzymes in the three strains (Fig. 1F). No appreciable difference in urea level was seen amongst the three strains (Fig. S1B), although WSB-db mice had considerably lower creatinine levels than WSB and B6-db animals (Fig. 1G). In comparison to WSB and B6-db mice, WSB-db mice had a significant increase in lymphocyte count and a decrease in monocyte and granulocyte count (Fig. S1C). This could be a result of persistent reactive leukocytosis brought on by weight gain.[4]

Peer review under responsibility of Chongqing Medical University.

https://doi.org/10.1016/j.gendis.2023.04.020

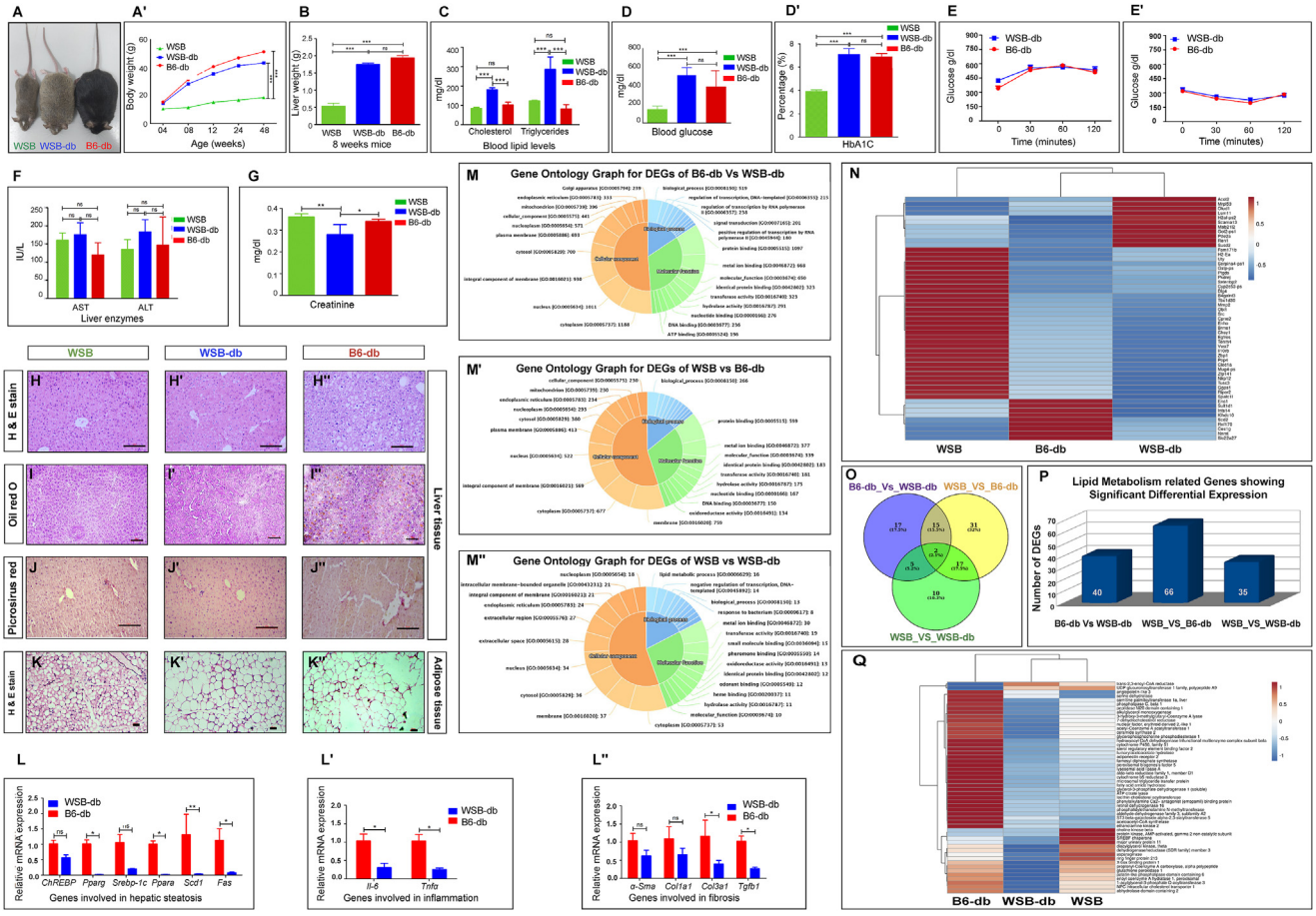

Figure 1 *Lepr* mutation from db/db in the WSB/Eij background causes the new congenic WSB-db mice to develop obesity but not NAFLD. **(A)** The representative image showing an animal of the recipient (WSB), congenic (WSB-db), and the *Lepr* mutation donor (B6-db) strains. **(A′)** Body weight of animals of each of the three strains (WSB, WSB-db, and B6-db) from 4 weeks to 48 weeks ($n = 5$). **(B)** Mean liver weight of animals of each of the three strains at the end of 8 weeks ($n = 5$). Graphical representation of serum biochemistry analyses for **(C)** cholesterol and triglycerides, **(D)** glucose, **(D″)** glycated hemoglobin (HbA1c) in the three strains, glucose tolerance test **(E)** and insulin tolerance test **(E′)** performed in B6-db and WSB-db mice, and serum biochemistry analyses for **(F)** alanine aminotransferase and aspartate aminotransferase, and **(G)** creatinine, from animals of the three strains. Liver tissue sections of animals from the three strains stained by **(H—H″)** hematoxylin/eosin, **(I—I″)** oil O red, and **(J—J″)** picrosirius red. No fibrosis was seen in the portal/periportal region in WSB and WSB-db mice. Mild periportal fibrosis was observed in B6-db mice. **(K—K″)** Hematoxylin/eosin-stained adipose tissue sections from the three strains. Bar graphs show relative mRNA expression of genes involved in hepatic steatosis, (L′) inflammation and (L″) fibrosis in WSB-db and B6-db mice. **(M—M″)** Gene ontology for differentially expressed genes (DEGs) from pair-wise control case comparisons for **(M)** B6-db *vs* WSB-db, **(M′)** WSB *vs* B6-db, and **(M″)** WSB *vs* WSB-db. **(N)** The Heat map showing genes with altered expression identified by RNA-seq analysis in the WSB, B6-db, and WSB-db mice. **(O)** Venn diagram showing the number of lipid metabolism pathway-specific candidate genes obtained, and the extent of overlap in the RNA-Seq results from the 3 different types of control-case comparisons (B6-db *vs* WSB-db, WSB *vs* B6-db, and WSB *vs* WSB-db). **(P)** Graphical summary of DEGs between 3 pair-wise control—case groups, belonging to the lipid metabolism pathways. **(Q)** The Heat map demonstrating the hierarchical clustering of the lipid metabolism-specific DEGs in the B6-db, WSB-db, and WSB.

Histopathological analysis of B6-db mouse liver sections revealed ballooning hepatocytes as well as micro- and macro-vesicular fat degeneration, confirming steatosis in B6-db animals only (Fig. 1H—H"). Compared to B6-db mice, WSB-db mice had fewer lipid droplets (Fig. 1I—I"). There was no discernible collagen deposition/fibrosis in the portal/periportal region of WSB-db (Fig. 1 J′) or WSB mice (Fig. 1J). However, B6-db mice showed mild periportal fibrosis (Fig. 1J"). Adipose tissue from WSB mice had normal morphology, as opposed to WSB-db mice, which had few annular adipocytes with infiltration by lymphocytes at the edges in B6-db mice (Fig. 1K—K"). The renal parenchyma of both WSB (Fig. S2A) and WSB-db (Fig. S2A′) had normal glomerular and tubular morphology but showed slight pigmentation of tubular epithelial cells in B6-db mice (Fig. S2A″). The pancreas of WSB mice had normal beta and acinar cells (Fig. S2B), whereas in WSB-db mice moderate islet hypertrophy with beta cell hyperplasia (Fig. S2B′) was

Table 1 Genes upregulated in WSB mice.

B4galnt3	beta-1,4-N-acetyl-galactosaminyl transferase 3
Brms1	breast cancer metastasis-suppressor 1
Clec1a	C-type lectin domain family 1, member a
Chsy1	chondroitin sulfate synthase 1
Cpne2	copine II
Dlg4	discs large MAGUK scaffold protein 4
Enho	energy homeostasis associated
Ggps1	geranylgeranyl diphosphate synthase 1
Gstp-ps	glutathione S-transferase, pi, pseudogene
H2-Ea	histocompatibility 2, class II antigen E alpha
Mug4-ps	murinoglobulin 4, pseudogene
Nnmt	nicotinamide N-methyltransferase
Nlrp12	NLR family, pyrin domain containing 12
Pkdrej	polycystin (PKD) family receptor for egg jelly
Pop4	processing of precursor 4, ribonuclease P/MRP family, (*S. cerevisiae*)
Ptgds	prostaglandin D2 synthase (brain)
Tbc1d30	TBC1 domain family, member 30
Tenm4	teneurin transmembrane protein 4
Tusc3	tumor suppressor candidate 3
Uty	ubiquitously transcribed tetratricopeptide repeat containing, Y-linked
Vwa7	von Willebrand factor A domain containing 7
Zbp1	Z-DNA binding protein 1
Zfp141	zinc finger protein 141

Table 1 Genes upregulated in DB.WSB mice.

Acot2	acyl-CoA thioesterase 2
Got2-ps1	glutamatic-oxaloacetic transaminase 2, mitochondrial, pseudogene 1
H2af-ps2	H2A histone family, pseudogene 2
Mab21l2	mab-21-like 2
Otud1	OTU domain containing 1
Pde2a	phosphodiesterase 2A, cGMP-stimulated
Ren1	renin 1 structural
Susd2	sushi domain containing 2
Lsm11	U7 snRNP-specific Sm-like protein LSM11

Table 1 Upregulated and Dounregulated genes among the groups:

	Upregulated genes	Downregulated genes
WSB *vs* DB. WSB	Apoe, Acaa1b, Acot8, Acot2, Acot3, Pck1, Thrsp, Acot4, B4galt6, Ces1d, Ces1g, Cyp26b1, Etnk2, Acot1, Sult2a1	Aldh3a2, Dhdds, Ggps1, Chka, Cyp2u1, Lrat, Far1, Hsd17b2, Hsd3b5, Elovl3, Gstp1, Hsd3b2, Mup11, Mup19, Mup18, Mup16, Mup9, Plcxd2, Mup12
WSB *vs* DB	Pparg, Aldh3a2, Acaa1b,Fads1, Pltp, Cyb5r3, Sgpp1, Acot3, Elovl2, Hmgcr, Rida, Sqle, Trem2, Tm7sf2, Vldlr, Cyp2c40, Scd2, Lpgat1, Hsd17b7, Cers6,Slc27a2, Ptgr1, Gpat3, Aacs, Adipor2, Far2,Acpp, B3galt2,Thrsp,Scd1, Acer2,Elovl6, Pnpla3,Acacb, Cyp2c37 Pgp, Insig1, Fitm2, Ptges,Cbr1,Plpp2,Acot4,Lipg, B4galt6,Retsat, Ces1d,Ces1g,Chpt1 Ces2c, Etnk2, Sult2a1	Ptgds, Dgka Hsd17b6 Mup16, Inpp5d, Cyp2u1,Hsd3b5, Elovl3, St6galnac3, Mup11, Mup19, Mup18, Mup9,Mup12
DB *vs* DB.WSB	Apoe, Cyp2c39, Dgka, Cyp2u1, Ugt1a9	Pltp, Cyb5r3, Acot2, Ggps1, Elovl2, Hmgcr, Dnajc15, Fitm1, Trem2, Cyp2c40 Scd2, Echs1, Lypla1, Lpgat1, Lrat, Hacd4, Prkaa2,Sult1d1,Cds1, Etnk1 Cyp2r1, Acpp, B3galt2, Plcg2,Acot11, Pnpla8, Scd1,Osbpl10, Acacb Cyp2c37, Sptssa,Chpt1,Hsd3b2,Sult2a1

Table 1 Upregulated and downregulated genes specific to the lipid metabolism pathways among the three strains, based on the heat map

Upregulated genes in WSB/EiJ mice compared to the other two strains	Chkb, Prkag2, Scap, Aspg, Rnf213, Ugt1a9
Downregulated Genes in WSB/EiJ mice compared to other strains	Pemt, Aldh3a2, Angptl3, Aacs,Sds,Ebp, Faah, Lcat, St3gal5, Rdh16, Etnk2
Downregulated Genes in WSB.DB mice compared with the other two strains	Agpat3, Cyp51, Pnpla6, Dgkq, Pex5, Cers2, Cyb5r3, Xbp1, Acly, Srebf2, Chkb, Gpd1, Npc1, Lipa, Cpt1a, Gpcpd1, Mttp, Hmgcl, Adipor2, Fah, Acat1.Scap, Faah, Lcat, Aspg, Nfe2l1, Akr1d1, Abhd2, Pcca, Pm20d1, Agmo, Plcb1, Ech1, hcr7, Hadhb, Fdps, Gpx1, Dhrs3, Mup11
Up regulated Genes in WSB.DB compared to other two strains	Tecr

seen. Thus, the histopathological evaluation confirmed that WSB-dbcongenic mice seem resistant to hepatic steatosis or other pathological changes in the liver.

Quantitation of expression levels of the genes involved in liver steatosis (Fig. 1L), inflammation (Fig. 1L′), and fibrosis (Fig. 1L′′) shows many of these genes have higher expression in B6-db mice as compared to WSB-db mice. Further, detailed liver transcriptome analysis was carried out for three control—case groups, WSB (control) *vs*. B6-db (case), WSB (control) *vs*. WSB-db (case), and B6-db (control) *vs*. WSB-db (case). Gene ontology and filtered genes for the three groups were mapped for biological process, molecular function, and cellular component (Fig. 1M—M′′; File S2). Interestingly, 53 DEGs were common to each of the three strains and are represented in the heat map (Fig. 1N; File S3). Based on the heat map, the up-regulated and downregulated genes among the three groups are presented in Table S1. Since the WSB-db mice develop dietary obesity but not NAFLD, we extracted DEGs involved in the lipid metabolic process (GO 006629) and analyzed the three control—case groups for significant genes using data based on the log fold change. In each group, the lipid metabolism-specific DEGs with upregulated and downregulated expression are summarized in Figure 1O, P, Table S1, and File S4. Among the DEGs of the lipid metabolic process, 52 genes were expressed in all three strains (Fig. 1Q; File S5). Finally, the interactive gene network analysis of lipid metabolism-specific genes from the RNA-seq data identified gene networks (Fig. S3) that could provide leads for understanding their differential roles in susceptibility to obesity and resistance to NAFLD in the new congenic WSB-db strain compared to the parental strains (WSB and B6-db).

The ob/ob and db/db mouse strains elicit phenotypic differences between severe obesity versus severe diabetes, only when maintained on the C57BL/6J and C57BLKS/J genetic backgrounds, respectively.[2,3] However, when maintained on the same genetic background, both *Lep* (ob/ob) or *Lepr* (db/db) deficiency results in almost identical phenotypes.[5] This demonstrates the importance of interaction between the genetic mutations and genetic background in manifesting complex disorders. Previous research on NAFLD mostly used animal models where NAFLD was induced and then the liver transcriptome was analyzed. Our study is distinct because we introduced the *Lepr* (db) mutation in the WSB strain which is uniquely resistant to obesity, T2DM, and NAFLD, compared to the other wild-derived strains such as CAST and PWK. Notably, this congenic WSB-db strain carrying the *Lepr* (db) mutation showed a significant shift in disease susceptibility compared to the WSB parent strain and displayed only a monogenic pattern of moderate obesity with diabetes. The WSB-db congenic strain may therefore serve as an appropriate model to elucidate the molecular basis of the pathogenic trio of obesity, NAFLD, and T2DM.

For insights into the more subtle differences between the pathophysiology of obesity and NAFLD, future investigations on the new congenic WSB-db strain using comparatively higher animal numbers and functional characterization of the genes identified in the current and prospective datasets are needed .

Author contributions

P.N. conceived and designed the study. S.A. performed experiments. P.N. and MJ.M.K. performed the pathological evaluation. P.N. and M.S. discussed and interpreted the results. P.N., M.S., and MJ.M.K. prepared the manuscript. All authors read and approved the final manuscript.

Conflict of interests

All authors declare that they have no conflict of interests.

Funding

The authors thank the Director of, the National Institute of Immunology (NII), New Delhi, and the Department of Biotechnology, India for funding. MS is funded currently by a DBT/Wellcome Trust India Alliance, India (IA/E/16/1/503028).

Acknowledgements

The authors wish to thank Mr. Subash Dogra Small Animal Facility (SAF), and the National Institute of Immunology for technical help in this study.

Appendix A. Supplementary data

Supplementary data to this article can be found online at https://doi.org/10.1016/j.gendis.2023.04.020.

References

1. Riazi K, Azhari H, Charette JH, et al. The prevalence and incidence of NAFLD worldwide: a systematic review and meta-analysis. *Lancet Gastroenterol Hepatol*. 2022;7(9):851—861.
2. Kleinert M, Clemmensen C, Hofmann SM, et al. Animal models of obesity and diabetes mellitus. *Nat Rev Endocrinol*. 2018;14(3):140—162.
3. Jahn D, Kircher S, Hermanns HM, Geier A. Animal models of NAFLD from a hepatologist's point of view. *Biochim Biophys Acta, Mol Basis Dis*. 2019;1865(5):943—953.
4. Herishanu Y, Rogowski O, Polliack A, Marilus R. Leukocytosis in obese individuals: possible link in patients with unexplained persistent neutrophilia. *Eur J Haematol*. 2006;76(6):516—520.
5. Coleman DL. Obese and diabetes: two mutant genes causing diabetes-obesity syndromes in mice. *Diabetologia*. 1978;14(3):141—148.

MJ Mahesh Kumar [b], Shailendra Arindkar [a], Masum Saini [c], Perumal Nagarajan [a,*]

[a] *National Institute of Immunology, New Delhi 100067, India*
[b] *Center for Cellular and Molecular Biology, Hyderabad 500007, India*
[c] *Regional Center for Biotechnology, Faridabad 121001, India*

*Corresponding author.
E-mail address: nagarajan@nii.ac.in (P. Nagarajan)

30 November 2022
Available online 21 June 2023